

# Isospin Dynamics in Heavy Ion Collisions: EoS-sensitive Observables

M.Di Toro<sup>a\*</sup>, V.Baran<sup>b</sup>, M.Colonna<sup>a</sup>, G.Ferini<sup>a</sup>, T.Gaitanos<sup>c</sup>, V.Greco<sup>a</sup>, J.Rizzo<sup>a</sup>,  
H.H.Wolter<sup>c</sup>.

<sup>a</sup>Laboratori Nazionali del Sud INFN, I-95123 Catania, Italy,  
and Physics-Astronomy Dept., University of Catania

<sup>b</sup>Dept.of Theoretical Physics, Bucharest Univ., Magurele, Bucharest, Romania

<sup>c</sup>Dept. für Physik, Universität München, D-85748 Garching, Germany

Heavy Ion Collisions (*HIC*) represent a unique tool to probe the in-medium nuclear interaction in regions away from saturation and at high nucleon momenta. In this report we present a selection of reaction observables particularly sensitive to the isovector part of the interaction, i.e. to the symmetry term of the nuclear Equation of State (*EoS*). At low energies the behavior of the symmetry energy around saturation influences dissipation and fragment production mechanisms. Predictions are shown for deep-inelastic and fragmentation collisions induced by neutron rich projectiles. Differential flow measurements will also shed lights on the controversial neutron/proton effective mass splitting in asymmetric matter. The high density symmetry term can be derived from isospin effects on heavy ion reactions at relativistic energies (few *AGeV* range), that can even allow a “direct” study of the covariant structure of the isovector interaction in the hadron medium. Rather sensitive observables are proposed from collective flows and from pion/kaon production. The possibility of the transition to a mixed hadron-quark phase, at high baryon and isospin density, is finally suggested. Some signatures could come from an expected “neutron trapping” effect.

## 1. Introduction

The symmetry energy  $E_{sym}$  appears in the energy density  $\epsilon(\rho, \rho_3) \equiv \epsilon(\rho) + \rho E_{sym} (\rho_3/\rho)^2 + O(\rho_3/\rho)^4 + \dots$ , expressed in terms of total ( $\rho = \rho_p + \rho_n$ ) and isospin ( $\rho_3 = \rho_p - \rho_n$ ) densities. The symmetry term gets a kinetic contribution directly from basic Pauli correlations and a potential part from the highly controversial isospin dependence of the effective interactions [1]. Both at sub-saturation and supra-saturation densities, predictions based of the existing many-body techniques diverge rather widely, see [2]. We take advantage of new opportunities in theory (development of rather reliable microscopic transport codes for *HIC*) and in experiments (availability of very asymmetric radioactive beams, improved possibility of measuring event-by-event correlations) to present results that are severely constraining the existing effective interaction models. We will discuss dissipative colli-

---

\*ditorio@lns.infn.it

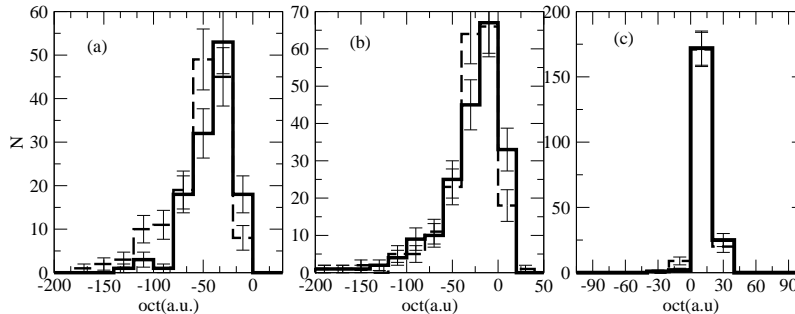


Figure 1. Distribution of the octupole moment of primary fragments for the  $^{132}\text{Sn} + ^{64}\text{Ni}$  reaction at 10  $A\text{MeV}$  (impact parameters (a):  $b = 6\text{fm}$ , (b):  $7\text{fm}$ , (c):  $8\text{fm}$ ). Solid lines: asysoft. Dashed lines: asystiff

sions in a wide range of energies, from just above the Coulomb barrier up to a few  $A\text{GeV}$ . The transport codes are based on mean field theories, with correlations included via hard nucleon-nucleon elastic and inelastic collisions and via stochastic forces, selfconsistently evaluated from the mean phase-space trajectory, see [ 1, 3, 4, 5]. Stochasticity is essential in order to get distributions as well as to allow the growth of dynamical instabilities.

## 2. Isospin effects on Deep-Inelastic Collisions

Dissipative semi-peripheral collisions at low energies, including binary and three-body breakings, offer a good opportunity to study phenomena occurring in nuclear matter under extreme conditions with respect to shape, excitation energy, spin and N/Z ratio (isospin). In some cases, due to a combined Coulomb and angular momentum (deformation) effect, some instabilities can show up [ 6]. This can lead to 3-body breakings, where a light cluster is emitted from the neck region. Three body processes in collisions with exotic beams will allow to investigate how the development of surface (neck-like) instabilities, that would help ternary breakings, is sensitive to the structure of the symmetry term around (below) saturation. In order to suggest proposals for the new *RIB* facility *Spiral 2*, [ 7] we have studied the reaction  $^{132}\text{Sn} + ^{64}\text{Ni}$  at 10  $A\text{MeV}$  in semicentral events, impact parameters  $b = 6, 7, 8\text{fm}$ , where one observes mostly binary exit channels, but still in presence of large dissipation. Two different behaviors of the symmetry energy below saturation have been tested: one (*asysoft*) where it is a smooth decreasing function towards low densities, and another one (*asystiff*) where we have a rapid decrease, [ 1]. The Wilczynski plots, kinetic energy loss vs. deflection angle, show slightly more dissipative events in the *asystiff* case, consistent with the point that in the interaction at lower densities in very neutron-rich matter (the neck region) we have a less repulsive symmetry term. In fact the neck dynamics is rather different in the two cases, as it can be well evidenced looking at the deformation of the *PLF/TLF* residues. The distribution of the octupole moment over the considered ensemble of events is shown in Fig.1 for the three considered impact parameters. Except for the most peripheral events, larger deformations, strongly suggesting a final 3-body outcome, are seen in the *asystiff* case. Now, due to the lower value of the symmetry energy, the neutron-rich neck connecting

the two systems survives a longer time leading to very deformed primary fragments, from which eventually small clusters will be dynamically emitted. Finally we expect to see effects of the different interaction times on the charge equilibration mechanism, probed starting from entrance channels with large  $N/Z$  asymmetries, like  $^{132}\text{Sn}(N/Z = 1.64) + ^{58}\text{Ni}(N/Z = 1.07)$ . Moreover the equilibration mechanism is also directly driven by the strenght of the symmetry term.

### 3. Isospin Dynamics in Neck Fragmentation at Fermi Energies

It is now quite well established that the largest part of the reaction cross section for dissipative collisions at Fermi energies goes through the *Neck Fragmentation* channel, with *IMFs* directly produced in the interacting zone in semiperipheral collisions on very short time scales [ 8]. We can predict interesting isospin transport effects for this new fragmentation mechanism since clusters are formed still in a dilute asymmetric matter but always in contact with the regions of the projectile-like and target-like remnants almost at normal densities. Since the difference between local neutron-proton chemical potentials is given by  $\mu_n - \mu_p = 4E_{\text{sym}}(\rho_3/\rho)$ , we expect a larger neutron flow to the neck clusters for a stiffer symmetry energy around saturation, [ 1, 9]. The isospin dynamics can be directly extracted from correlations between  $N/Z$ , *alignement* and emission times of the *IMFs*. The alignment between *PLF* – *IMF* and *PLF* – *TLF* directions represents a very convincing evidence of the dynamical origin of the mid-rapidity fragments produced on short time scales [ 10]. The form of the  $\Phi_{\text{plane}}$  distributions (centroid and width) can give a direct information on the fragmentation mechanism [ 11]. Recent calculations confirm that the light fragments are emitted first, a general feature expected for that rupture mechanism [ 12]. The same conclusion can be derived from *direct* emission time measurements based on deviations from Viola systematics observed in event-by-event velocity correlations between *IMFs* and the *PLF/TLF* residues [ 10, 11, 13]. We can figure out a continuous transition from fast produced fragments via neck instabilities to clusters formed in a dynamical fission of the projectile(target) residues up to the evaporated ones (statistical fission). Along this line it would be even possible to disentangle the effects of volume and shape instabilities. A neutron enrichment of the overlap ("neck") region is expected, due to the neutron migration from higher (spectator) to lower (neck) density regions, directly related to the slope of the symmetry energy [ 12]. A very nice new analysis has been presented on the  $\text{Sn} + \text{Ni}$  data at 35 *AMeV* by the Chimera Collab., Fig.2 of ref.[ 14]. A strong correlation between neutron enrichment and alignment (when the short emission time selection is enforced) is seen, that can be reproduced only with a stiff behavior of the symmetry energy. *This is the first clear evidence in favor of a relatively large slope (symmetry pressure) around saturation.*

### 4. Effective Mass Splitting and Collective Flows

The problem of Momentum Dependence in the Isovector channel (*Iso* – *MD*) is still very controversial and it would be extremely important to get more definite experimental information, see the recent refs. [ 15, 16, 17, 18, 19, 20]. Intermediate energies are important in order to have high momentum particles and to test regions of high baryon (isoscalar) and isospin (isovector) density during the reactions dynamics. Collective flows

[ 21] are very good candidates since they are expected to be very sensitive to the momentum dependence of the mean field, see [ 22, 1]. The transverse flow,  $V_1(y, p_t) = \langle \frac{p_x}{p_t} \rangle$ , provides information on the anisotropy of nucleon emission on the reaction plane. Very important for the reaction dynamics is the elliptic flow,  $V_2(y, p_t) = \langle \frac{p_x^2 - p_y^2}{p_t^2} \rangle$ . The sign of  $V_2$  indicates the azimuthal anisotropy of emission: on the reaction plane ( $V_2 > 0$ ) or out-of-plane (*squeeze - out*,  $V_2 < 0$ ) [ 21, 22]. We have then tested the *Iso - MD* of the fields just evaluating the *Difference* of neutron/proton transverse and elliptic flows  $V_{1,2}^{(n-p)}(y, p_t) \equiv V_{1,2}^n(y, p_t) - V_{1,2}^p(y, p_t)$  at various rapidities and transverse momenta in semicentral ( $b/b_{max} = 0.5$ )  $^{197}\text{Au} + ^{197}\text{Au}$  collisions at 250 A MeV, where some proton data are existing from the *FOPI* collaboration at *GSI* [ 23, 24]. The transport code has been implemented with a *BGBD - like* [ 25, 26] mean field with a different  $(n, p)$  momentum dependence, see [ 16, 17, 18], that allow to follow the dynamical effect of opposite n/p effective mass splitting while keeping the same density dependence of the symmetry energy.

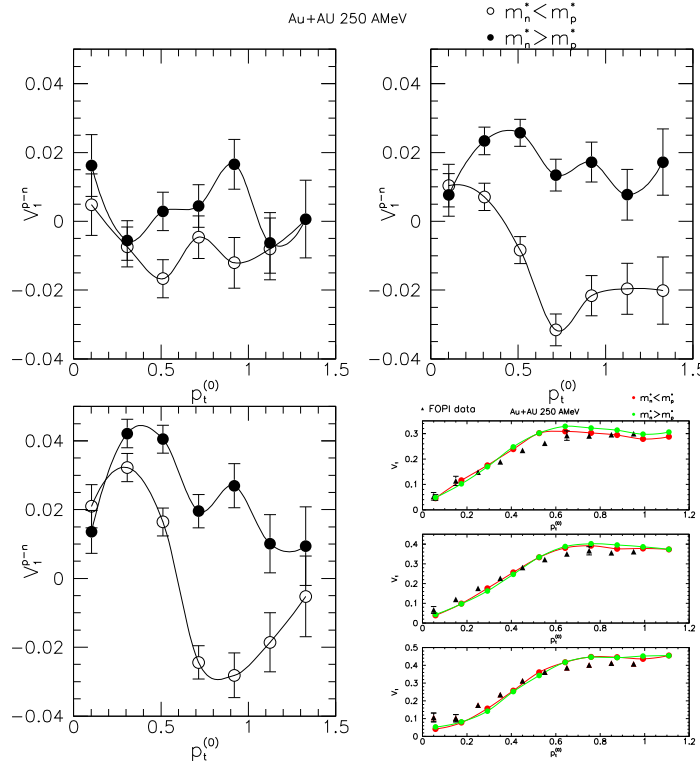


Figure 2. Difference between proton and neutron  $V_1$  flows in a semi-central reaction Au+Au at 250 A MeV for three rapidity ranges. Upper Left Panel:  $|y^{(0)}| \leq 0.3$ ; Upper Right:  $0.3 \leq |y^{(0)}| \leq 0.7$ ; Lower Left:  $0.6 \leq |y^{(0)}| \leq 0.9$ . Lower Right Panel: Comparison of the  $V_1$  proton flow with FOPI data [ 23] for three rapidity ranges. Top:  $0.5 \leq |y^{(0)}| \leq 0.7$ ; center:  $0.7 \leq |y^{(0)}| \leq 0.9$ ; bottom:  $0.9 \leq |y^{(0)}| \leq 1.1$ .

For the difference of nucleon transverse flows, see Fig. 2, the mass splitting effect is evident at all rapidities, and nicely increasing at larger rapidities and transverse momenta, with more neutron flow when  $m_n^* < m_p^*$ . Just to show that our simulations give realistic results we compare in lower right panel of Fig. 2 with the proton data of the *FOPI* collaboration for similar selections of impact parameters rapidities and transverse

momenta. The same analysis has been performed for the difference of elliptic flows, [17]. Again the mass splitting effects are more evident for higher rapidity and transverse momentum selections. In particular the differential elliptic flow becomes negative when  $m_n^* < m_p^*$ , revealing a faster neutron emission and so more neutron squeeze out (more spectator shadowing). The measurement of n/p flow differences appears essential. Due to the difficulties in measuring neutrons, our suggestion is to measure the difference between light isobar flows, like  ${}^3H$  vs.  ${}^3He$  and so on. We expect to clearly see the effective mass splitting effects, maybe even enhanced due to larger overall flows shown by clusters, see [1, 27].

## 5. Relativistic Collisions

Finally we focus our attention on relativistic heavy ion collisions, that provide a unique terrestrial opportunity to probe the in-medium nuclear interaction at high densities. An effective Lagrangian approach to the hadron interacting system is extended to the isospin degree of freedom: within the same frame equilibrium properties (*EoS*, [28]) and transport dynamics [29, 30] can be consistently derived. Within a covariant picture of the nuclear mean field, for the description of the symmetry energy at saturation ( $a_4$  parameter of the Weizsäcker mass formula) (a) only the Lorentz vector  $\rho$  mesonic field, and (b) both, the vector  $\rho$  (repulsive) and scalar  $\delta$  (attractive) effective fields [31, 32] can be included. In the latter case the competition between scalar and vector fields leads to a stiffer symmetry term at high density [31, 1]. The presence of the hadronic medium leads to effective masses and momenta  $M^* = M + \Sigma_s$ ,  $k^{*\mu} = k^\mu - \Sigma^\mu$ , with  $\Sigma_s$ ,  $\Sigma^\mu$  scalar and vector self-energies. For asymmetric matter the self-energies are different for protons and neutrons, depending on the isovector meson contributions. We will call the corresponding models as  $NL\rho$  and  $NL\rho\delta$ , respectively, and just  $NL$  the case without isovector interactions.

For the description of heavy ion collisions we solve the covariant transport equation of the Boltzmann type [29, 30] within the Relativistic Landau Vlasov (*RLV*) method, using phase-space Gaussian test particles [33], and applying a Monte-Carlo procedure for the hard hadron collisions. The collision term includes elastic and inelastic processes involving the production/absorption of the  $\Delta(1232MeV)$  and  $N^*(1440MeV)$  resonances as well as their decays into pion channels, [34, 35]. A larger repulsive vector contribution to the neutron energies is given by the  $\rho$ -coupling. This is rapidly increasing with density when the  $\delta$  field is included [31, 1]. As a consequence we expect a good sensitivity to the covariant structure of the isovector fields in nucleon emission and particle production data. Moreover the presence of a *Lorentz magnetic* term in the relativistic transport equation [29, 30, 1] will enhance the dynamical effects of vector fields [36].

Differential flows will be directly affected. In Fig.3 transverse and elliptic differential flows are shown for the  ${}^{132}Sn + {}^{124}Sn$  reaction at 1.5 AGeV ( $b = 6fm$ ), [36]. The effect of the different structure of the isovector channel is clear. Particularly evident is the splitting in the high  $p_t$  region of the elliptic flow. In the  $(\rho + \delta)$  dynamics the high- $p_t$  neutrons show a much larger *squeeze-out*. This is fully consistent with an early emission (more spectator shadowing) due to the larger  $\rho$ -field in the compression stage.

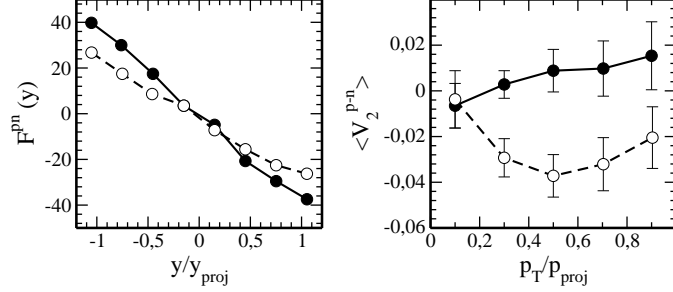


Figure 3. Differential neutron-proton flows for the  $^{132}\text{Sn} + ^{124}\text{Sn}$  reaction at 1.5 AGeV ( $b = 6\text{fm}$ ) from the two different models for the isovector mean fields. Left: Transverse Flows. Right: Elliptic Flows. Full circles and solid line:  $NL\rho\delta$ . Open circles and dashed line:  $NL\rho$ .

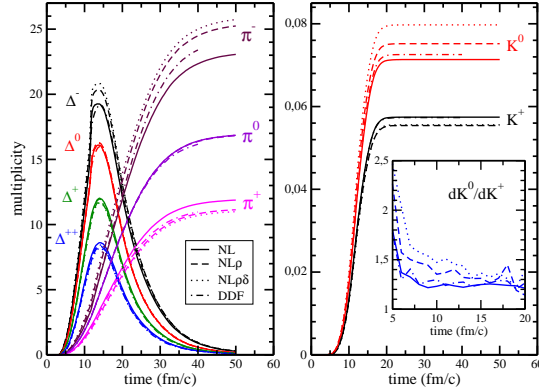


Figure 4. Time evolution of the  $\Delta^{\pm,0,++}$  resonances and pions  $\pi^{\pm,0}$  (left), and kaons ( $K^{\pm,0}$ ) (right) for a central ( $b = 0\text{ fm}$  impact parameter) Au+Au collision at 1 AGeV incident energy. Transport calculation using the  $NL$ ,  $NL\rho$ ,  $NL\rho\delta$  and  $DDF$  models for the iso-vector part of the nuclear  $EoS$  are shown.

## 6. Isospin effects on sub-threshold kaon production at intermediate energies

Kaon production has been proven to be a reliable observable for the high density  $EoS$  in the isoscalar sector [37, 38]. Here we show that the  $K^0/K^+$  production (in particular the  $K^0/K^+$  yield ratio) can be also used to probe the isovector part of the  $EoS$ .

Using our  $RMF$  transport approach we analyze pion and kaon production in central  $^{197}\text{Au} + ^{197}\text{Au}$  collisions in the 0.8 – 1.8 AGeV beam energy range, comparing models giving the same “soft”  $EoS$  for symmetric matter and with different effective field choices for  $E_{sym}$  [35]. Here we also use a Lagrangian with density dependent couplings ( $DDF$ , [32]), recently suggested for better nucleonic properties of neutron stars [39]. In the  $DDF$  model the  $\rho$ -coupling is exponentially decreasing with density, resulting in a rather “soft” symmetry term at high density. The hadron mean field propagation, which goes beyond the “collision cascade” picture, is essential for particle production yields: in particular the isospin dependence of the self-energies directly affects the energy balance of the inelastic channels.

Fig. 4 reports the temporal evolution of  $\Delta^{\pm,0,++}$  resonances, pions ( $\pi^{\pm,0}$ ) and kaons ( $K^{\pm,0}$ ) for central Au+Au collisions at 1 AGeV. It is clear that, while the pion yield freezes out at times of the order of 50 fm/c, i.e. at the final stage of the reaction (and at low densities), kaon production occur within the very early (compression) stage, and the

yield saturates at around  $20 fm/c$ . From Fig. 4 we see that the pion results are weakly dependent on the isospin part of the nuclear mean field. However, a slight increase (decrease) in the  $\pi^-$  ( $\pi^+$ ) multiplicity is observed when going from the  $NL$  (or  $DDF$ ) to the  $NL\rho$  and then to the  $NL\rho\delta$  model, i.e. increasing the vector contribution  $f_\rho$  in the isovector channel. This trend is more pronounced for kaons, see the right panel, due to the high density selection of the source and the proximity to the production threshold.

When isovector fields are included the symmetry potential energy in neutron-rich matter is repulsive for neutrons and attractive for protons. In a *HIC* this leads to a fast, pre-equilibrium, emission of neutrons. Such a *mean field* mechanism, often referred to as isospin fractionation [1], is responsible for a reduction of the neutron to proton ratio during the high density phase, with direct consequences on particle production in inelastic  $NN$  collisions. *Threshold* effects represent a more subtle point. The energy conservation in a hadron collision is expressed in terms of the canonical momenta, i.e. for a reaction  $1 + 2 \rightarrow 3 + 4$  as  $s_{in} = (k_1^\mu + k_2^\mu)^2 = (k_3^\mu + k_4^\mu)^2 = s_{out}$ . Since hadrons are propagating with effective (kinetic) momenta and masses, an equivalent relation should be formulated starting from the effective in-medium quantities  $k^{*\mu} = k^\mu - \Sigma^\mu$  and  $m^* = m + \Sigma_s$ , where  $\Sigma_s$  and  $\Sigma^\mu$  are the scalar and vector self-energies. The self-energy contributions will influence the particle production at the level of thresholds as well as of the phase space available in the final channel. In neutron-rich colliding systems *Mean field* and *threshold* effects are acting in opposite directions. At low energies, around the production threshold, the energy conservation (i.e. the self energy contributions) is dominant, as we see from Fig. 4, in particular for kaons.

We have to note that in a previous study of kaon production in excited nuclear matter the dependence of the  $K^0/K^+$  yield ratio on the effective isovector interaction appears much larger (see Fig.8 of ref.[34]). The point is that in the non-equilibrium case of a heavy ion collision the asymmetry of the source where kaons are produced is in fact reduced by the  $n \rightarrow p$  “transformation”, due to the favored  $nn \rightarrow p\Delta^-$  processes. This effect is almost absent at equilibrium due to the inverse transitions. Moreover in infinite nuclear matter even the fast neutron emission is not present. This result clearly shows that chemical equilibrium models can lead to uncorrect results when used for transient states of an *open* system.

## 7. Testing Deconfinement at High Isospin Density

The hadronic matter is expected to undergo a phase transition into a deconfined phase of quarks and gluons at large densities and/or high temperatures. On very general grounds, the transition critical densities are expected to depend on the isospin of the system, but no experimental tests of this dependence have been performed so far. In order to check the possibility of observing some precursor signals of some new physics even in collisions of stable nuclei at intermediate energies we have performed some event simulations for the collision of very heavy, neutron-rich, elements. We have chosen the reaction  $^{238}U + ^{238}U$  (average proton fraction  $Z/A = 0.39$ ) at  $1 AGeV$  and semicentral impact parameter  $b = 7 fm$  just to increase the neutron excess in the interacting region. After about  $10 fm/c$  in the overlap region a nice local equilibration is achieved. A rather exotic nuclear matter is formed in a transient time of the order of  $10 fm/c$ , with baryon density

around  $3 - 4\rho_0$ , temperature  $50 - 60 \text{ MeV}$ , energy density  $\approx 500 \text{ MeV fm}^{-3}$  and proton fraction between 0.35 and 0.40, likely inside the estimated mixed phase region [40].

We can study the isospin dependence of the transition densities [41] in a systematic way. Concerning the hadronic phase, we use the relativistic non-linear model of Glendenning-Moszkowski (in particular the “soft” *GM3* choice) [42], where the isovector part is treated just with  $\rho$  meson coupling, and the iso-stiffer *NL $\rho\delta$*  interaction [40]. For the quark phase we consider the *MIT* bag model with various bag pressure constants. In particular we are interested in those parameter sets which would allow the existence of quark stars [43], i.e. parameter sets for which the so-called Witten-Bodmer hypothesis is satisfied [44, 45]. One of the aim of our work it to show that if quark stars are indeed possible, it is then very likely to find signals of the formation of a mixed quark-hadron phase in intermediate-energy heavy-ion experiments [40]. The structure of the mixed phase is obtained by imposing the Gibbs conditions [46] for chemical potentials and pressure and by requiring the conservation of the total baryon and isospin densities

$$\begin{aligned} \mu_B^{(H)} &= \mu_B^{(Q)}, \quad \mu_3^{(H)} = \mu_3^{(Q)}, \quad P^{(H)}(T, \mu_{B,3}^{(H)}) = P^{(Q)}(T, \mu_{B,3}^{(Q)}), \\ \rho_B &= (1 - \chi)\rho_B^H + \chi\rho_B^Q, \quad \rho_3 = (1 - \chi)\rho_3^H + \chi\rho_3^Q, \end{aligned} \quad (1)$$

where  $\chi$  is the fraction of quark matter in the mixed phase. In this way we get the *binodal* surface which gives the phase coexistence region in the  $(T, \rho_B, \rho_3)$  space [46, 41]. For a fixed value of the conserved charge  $\rho_3$  we will study the boundaries of the mixed phase region in the  $(T, \rho_B)$  plane. In the hadronic phase the charge chemical potential is given by  $\mu_3 = 2E_{sym}(\rho_B) \frac{\rho_3}{\rho_B}$ . Thus, we expect critical densities rather sensitive to the isovector channel in the hadronic *EoS*.

In Fig. 5 we show the crossing density  $\rho_{cr}$  separating nuclear matter from the quark-nucleon mixed phase, as a function of the proton fraction  $Z/A$ . We can see the effect of the  $\delta$ -coupling towards an *earlier* crossing due to the larger symmetry repulsion at high baryon densities. In the same figure we report the paths in the  $(\rho, Z/A)$  plane followed in the c.m. region during the collision of the n-rich  $^{132}\text{Sn} + ^{132}\text{Sn}$  system, at different energies. At  $300 \text{ AMeV}$  we are just reaching the border of the mixed phase, and we are well inside it at  $1 \text{ AGeV}$ . Statistical fluctuations could help in reducing the density at which drops of quark matter form. The reason is that a small bubble can be energetically favored if it contains quarks whose  $Z/A$  ratio is *smaller* than the average value of the surrounding region [40]. This corresponds to a *neutron trapping* effect, supported also by a symmetry energy difference in the two phases. In fact while in the hadron phase we have a large neutron potential repulsion (in particular in the *NL $\rho\delta$*  case), in the quark phase we only have the much smaller kinetic contribution. If in a pure hadronic phase neutrons are quickly emitted or “transformed” in protons by inelastic collisions, when the mixed phase starts forming, neutrons are kept in the interacting system up to the subsequent hadronization in the expansion stage [40]. Observables related to such neutron “trapping” could be an inversion in the trend of the formation of neutron rich fragments and/or of the  $\pi^-/\pi^+$ ,  $K^0/K^+$  yield ratios for reaction products coming from high density regions, i.e. with large transverse momenta.



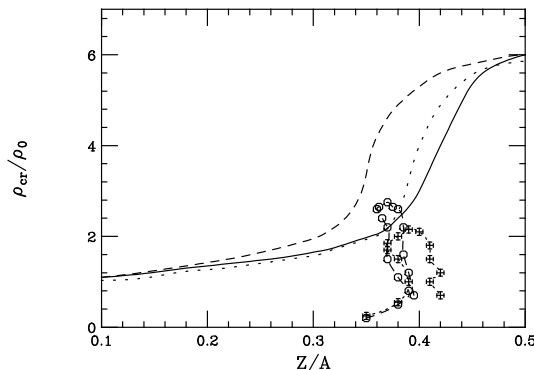


Figure 5. Variation of the transition density with proton fraction for various hadronic *EoS* parameterizations. Dotted line: *GM3* parametrization; dashed line: *NL* $\rho$  parametrization; solid line: *NL* $\rho\delta$  parametrization. For the quark *EoS*, the *MIT* bag model with  $B^{1/4}=150$  MeV. The points represent the path followed in the interaction zone during a semi-central  $^{132}\text{Sn}+^{132}\text{Sn}$  collision at 1 AGeV (circles) and at 300 AMeV (crosses).

## 8. Perspectives

We have shown that *violent* collisions of n-rich heavy ions from low to relativistic energies can bring new information on the isovector part of the in-medium interaction, qualitatively different from equilibrium *EoS* properties. We have presented quantitative results in a wide range of beam energies. At low energies we have shown isospin effects on the dissipation in deep inelastic collisions, at Fermi energies the Iso-*EoS* sensitivity of the isospin transport in fragment reactions and finally at intermediate the dependence of differential flows on the *Iso*–*MD* and effective mass splitting. In relativistic collisions we have shown the possibility of a direct *measure* of the Lorentz structure of the isovector fields at high baryon density, from differential collective flows and yields of charged pion and kaon ratios. Important non-equilibrium effects for particle production are stressed. Finally our study supports the possibility of observing precursor signals of the phase transition to a mixed hadron-quark matter at high baryon density in the collision, central or semi-central, of neutron-rich heavy ions in the energy range of a few AGeV. As signatures we suggest to look at the isospin structure of hadrons produced at high transverse momentum, as a good indicator of the neutron trapping effect. In conclusion the results presented here appear very promising for the possibility of exciting new results from dissipative collisions with radioactive beams.

### Acknowledgements

We warmly thanks A.Drago and A.Lavagno for the intense collaboration on the mixed hadron-quark phase transition at high baryon and isospin density.

## REFERENCES

1. V.Baran, M.Colonna, V.Greco, M.Di Toro, *Phys. Rep.* **410** (2005) 335.
2. C.Fuchs, H.H.Wolter, *Modelization of the EoS, nucl-th/0511070*, *Eur. Phys. Jour.* **A** 2006 in press
3. A.Guarnera, M.Colonna, P.Chomaz, *Phys. Lett.* **B373** (1996] 267.
4. M.Colonna et al., *Nucl. Phys.* **A642** (1998) 449.
5. P.Chomaz, M.Colonna, J.Randrup, *Phys. Rep.* **389** (2004) 263.

6. M.Colonna, M.Di Toro, A.Guarnera, *Nucl. Phys.* **A589** (1995) 160.
7. M.Lewitowicz, *Challenges of the SPIRAL 2 Project*, this volume..
8. M.Di Toro, A.Olmi, R.Roy, *Neck Dynamics*, *Eur. Phys. Jour. A* 2006 in press
9. V.Baran et al., *Phys. Rev.* **C72** (2005) 064620.
10. V.Baran, M.Colonna, M.Di Toro, *Nucl. Phys.* **A730** (2004) 329.
11. E.De Filippo et al. (Chimera Collab.), *Phys. Rev.* **C71** (2005) 044602; *Phys. Rev.* **C71** (2005) 064604.
12. R.Lionti, V.Baran, M.Colonna, M.Di Toro, *Phys. Lett.* **B625** (2005) 33.
13. J.Wilczynski et al. (Chimera Collab.), *Int. Jour. Mod. Phys.* **E14** (2005) 353.
14. E. De Filippo et al. (Chimera Collab.), *Time scales and isospin effects on reaction dynamics*, contribution in this volume.
15. B.-A. Li, B.Das Champak, S.Das Gupta, C.Gale, *Nucl. Phys.* **A735** (2004) 563.
16. J.Rizzo, M.Colonna, M.Di Toro, V.Greco, *Nucl. Phys.* **732** (2004) 202.
17. M.Di Toro, M.Colonna, J.Rizzo, *AIP Conf.Proc.* **791** (2005) 70-83
18. J.Rizzo, M.Colonna, M.Di Toro *Phys. Rev.* **C72** (2005) 064609.
19. W.Zuo, L.G.Cao, B.-A.Li, U.Lombardo, C.W.Shen, *Phys. Rev.* **C72** (2005) 014005.
20. E. van Dalen, C.Fuchs, A.Fässler, *Phys. Rev. Lett.* **95** (2005) 022302.
21. J.Y. Ollitrault, *Phys. Rev.* **D46** (1992) 229.
22. P. Danielewicz, *Nucl. Phys.* **A673** (2000) 375.
23. A.Andronic et al., FOPI Collab., *Phys. Rev.* **C67** (2003) 034907.
24. A.Andronic et al., FOPI Collab., *Phys. Lett.* **B612** (2005) 173.
25. C.Gale, G.F.Bertsch, S.Das Gupta, *Phys.Rev.* **C41** (1990) 1545.
26. I.Bombaci et al., *Nucl.Phys.* **A583** (1995) 623.
27. L.Scalone, M.Colonna, M.Di Toro, *Phys. Lett.* **B461** (1999) 9.
28. B. D. Serot, J. D. Walecka, *Advances in Nuclear Physics*, **16**, 1, eds. J. W. Negele, E. Vogt, (Plenum, N.Y., 1986).
29. C. M. Ko, Q. Li, R. Wang, *Phys. Rev. Lett.* **59** (1987) 1084.
30. B. Blättel, V. Koch, U. Mosel, *Rep. Prog. Phys.* **56** (1993) 1.
31. B. Liu, V. Greco, V. Baran, M. Colonna, M. Di Toro, *Phys. Rev.* **C65** (2002) 045201.
32. T. Gaitanos, et al., *Nucl. Phys.* **A732** (2004) 24.
33. C. Fuchs. H.H. Wolter, *Nucl. Phys.* **A589** (1995) 732.
34. G. Ferini, M. Colonna, T. Gaitanos, M. Di Toro, *Nucl. Phys.* **A762** (2005) 147.
35. G. Ferini et al., *Isospin effects on sub-threshold kaon production...*, *arXiv:nucl-th/0607005*.
36. V. Greco et al., *Phys. Lett.* **B562** (2003) 215.
37. C. Fuchs, *Prog.Part.Nucl.Phys.* **56** 1-103 (2006).
38. C.Hartnack, H.Oeschler, J.Aichelin, *Phys. Rev. Lett.* **96** (2006) 012302.
39. T.Klähn et al. *Constraints on the high-density...*, *arXiv:nucl-th/0602038*.
40. M. Di Toro, A. Drago, T. Gaitanos, V. Greco, A. Lavagno, *Nucl. Phys.* **A775** (2006) 102-126..
41. H.Mueller, *Nucl. Phys.* **A618** (1997) 349.
42. N.K.Glendenning, S.A.Moszkowski, *Phys. Rev. Lett.* **67** (1991) 2414.
43. A.Drago, A.Lavagno, *Phys. Lett.* **B511** (2001) 229.
44. E.Witten, *Phys. Rev.* **D30** (1984) 272.
45. A.R.Bodmer, *Phys. Rev.* **D4** (1971) 1601.

46. N.K.Glendenning, *Phys. Rev.* **D46** (1992) 1274.